catalysts

MDPI

Article

One-Step Biodiesel Production from Waste Cooking Oil Using CaO Promoted Activated Carbon Catalyst from *Prunus persica* Seeds

Ayesha Hameed [1], Salman Raza Naqvi [1,2], Umair Sikandar [1] and Wei-Hsin Chen [3,4,5,*]

[1] School of Chemical and Materials Engineering (SCME), National University of Sciences and Technology, Islamabad 44000, Pakistan; aashu.hameed265@gmail.com (A.H.); salman.raza@scme.nust.edu.pk (S.R.N.); umair.sikandar@scme.nust.edu.pk (U.S.)
[2] National Science & Technology Park, National University of Sciences and Technology, Islamabad 44000, Pakistan
[3] Department of Aeronautics and Astronautics, National Cheng Kung University, Tainan 701, Taiwan
[4] Research Center for Smart Sustainable Circular Economy, Tunghai University, Taichung 407, Taiwan
[5] Department of Mechanical Engineering, National Chin-Yi University of Technology, Taichung 411, Taiwan
* Correspondence: weihsinchen@gmail.com or chenwh@mail.ncku.edu.tw

Abstract: In recent years, the scope for replacing fossil fuels has been appealing to the world, owing to limited conventional fuels, crude oil price volatility, and greenhouse gas emission concerns. In this regard, this article demonstrates the preparation of a novel solid base catalyst for the transesterification of waste cooking oil. A calcium-loaded activated carbon catalyst was prepared through pyrolysis of peach shell followed by chemical activation with KOH and then calcium loading through the wet impregnation method. The prepared catalyst showed the best performance with 20% calcium loading and 650 °C of calcination temperature. The catalyst's physicochemical, structural, and textural properties were examined using XRD, FTIR, SEM, EDX, and BET analysis. The catalyst showed a maximum yield of 96% at optimized conditions, i.e., 65 °C temperature, oil to methanol ratio 1:8, 5 wt% catalyst concentration, and a 160 min reaction time. Additionally, it illustrated high recyclability up to 10 cycles with negligible leaching of Ca^{+2} ions. The high activity of the catalyst was due to the presence of calcium ions on the activated carbon support. Physio–chemical properties and GC-MS analysis of prepared biodiesel determined that all attributes were within the biodiesel standard tolerances set by ASTM D6751 and EN 14214. Therefore, all the innovations mentioned above concluded that catalyst generated from peach shell biochar is a promising candidate for biodiesel production, ultimately resulting in solid and liquid waste management.

Keywords: biodiesel; catalyst; peach shell; transesterification; waste cooking oil

check for updates

Citation: Hameed, A.; Naqvi, S.R.; Sikandar, U.; Chen, W.-H. One-Step Biodiesel Production from Waste Cooking Oil Using CaO Promoted Activated Carbon Catalyst from *Prunus persica* Seeds. *Catalysts* **2022**, *12*, 592. https://doi.org/10.3390/catal12060592

Academic Editor: Hoang Chinh Nguyen

Received: 24 April 2022
Accepted: 25 May 2022
Published: 30 May 2022

Publisher's Note: MDPI stays neutral with regard to jurisdictional claims in published maps and institutional affiliations.

Copyright: © 2022 by the authors. Licensee MDPI, Basel, Switzerland. This article is an open access article distributed under the terms and conditions of the Creative Commons Attribution (CC BY) license (https://creativecommons.org/licenses/by/4.0/).

1. Introduction

Recently, the production of clean natural energy sources has gained considerable interest as a consequence of increasing power consumption, fluctuating environmental conditions, and a growing reduction in available fuel-generating supplies [1–3]. Depletion of nonrenewable resources is at an all-time high, and they will soon be exhausted. Fossil fuel combustion also releases harmful pollutants into the environment, leading to a variety of other problems [4,5]. To deal with these issues, scholars worldwide are focusing their attention on this matter. Biodiesel, a first-generation biofuel, is becoming increasingly popular as a substitute for petroleum-based diesel all across the world [6,7]. In addition to biodiesel's biodegradability, technological feasibility, reduced greenhouse gas emissions (GHGs), nontoxicity, and carbon neutrality, biodiesel has several more benefits [8,9]. According to the estimation of biodiesel production, almost up to 80% of the total cost is shared by biodiesel feedstock, a blend of fatty acid methyl esters (FAME) is made from oil

feedstock such as vegetable oil, non-edible oil, waste cooking oil resources, animal fats, waxes and can be used without much alteration in diesel engines [10–12]. The development of biodiesel typically requires homogeneous catalysts such as (NaOH, KOH, and H_2SO_4) at the commercial level, leading to an elevated rate of reactions and reasonably moderate conditions [13–17]; however, such catalysts cannot be recovered or separated, and involve an expensive series of purification, recycling, and separation measures that produce significant volumes of wastewater, degradation of facilities, running costs, and high energy usage [18,19]. The advantages and efficiency of heterogeneous catalysts over homogeneous catalysts in the transesterification reaction have been commonly documented to solve such problems as they are less toxic, more stable, simpler to isolate, and eco-friendly in nature [20,21]. Scholars have already explored several specific catalysts which are heterogeneous in nature, such as alkali metals, alkaline earth metal oxides, supported metal catalysts, and simple zeolites for biodiesel production [22–27].

Biochar is a porous carbon-enriched material formed at a modest temperature by biomass pyrolysis with little to no accessible air [28–31]. Because of abundant feedstock, minimal expense, broad surface areas, and strong thermal stability, biochar is commonly used as a support or carbonaceous catalyst in biodiesel production [32–34]. Specifically, Zhao et al. [35] have experimentally synthesized catalysts based on biochar derived from waste pomelo peel loaded with K_2CO_3 to catalyze palm oil into biodiesel. Zhao et al. [36] found pyrolytic rice husk impregnated with CaO is an auspicious choice for the conversion of palm oil through the transesterification process. Wang et al. [37] proposed that the peat biochar has helped build economically strong base catalysts for the transesterification reaction. Chellappan et al. [38] experimentally tested green biochar-based Bronsted acid catalysts for both esterification and transesterification in biodiesel production.

Recently, a number of waste residues from agriculture, poultry, and households are being employed as feedstock for the profitable production of catalysts to effectively reduce the elevated costs of catalyst synthesis [39–43]. Calcium oxide (CaO) is one of the solid catalysts used in the transesterification of various feedstocks to biodiesel, a highly successful catalyst for biodiesel synthesis which has already been proven [44–46]; therefore, waste eggshells may also be a low-cost source for biodiesel processing. The waste eggshells comprise a significant amount of calcium compounds ($CaCO_3$) and can easily be transformed into CaO through high-temperature calcination. CaO is an inexpensive, environmentally safe, non-corrosive, eco-friendly, highly active substance under mild conditions that can be regenerated for another transesterification process [47–50], and such advantages attract the attention of other scientists for more research on the total properties of CaO.

Peach (*Prunus persica*) belongs to the family of Rosaceae, which was cultivated for more than 3000 years in China and has been distributed by seed to the rest of the planet [51]; it is the most significant among the stone fruits in nature. It is a typical crop of the northern Pakistan region and occupies 4543 hectares with 48,284 tons of production [52]. Quetta, Kalat, Peshawar, Swat Valley, and parts of the Kohistan Hills are the main rising region of peaches. Previously, the effects of peach biochar and organic residues, along with beneficial microbes and phosphorus, on the growth and productivity of soybeans and maize were measured, and it was concluded that peach biochar had a significant effect in increasing the overall use of phosphorus and the agronomic efficiency of crops [53]. Although, to date, carbon-based support for the development of a strong catalyst for the synthesis of biologic diesel has never been investigated. At present, there is much concern about the use of activated carbon loaded from various catalysts [54–57]. In addition to this, using a biochar-based green catalyst would help commercialize biodiesel production, and it also helps to promote the environmental feasibility of the pyrolysis process [58,59].

This research aims to leverage the high-performance, low-cost, and sustainable peach (*Prunus persica*) biochar assisted by the CaO catalyst for transesterification reactions. Additionally, potassium hydroxide (KOH) was used in this research for biochar activation to boost the catalytic efficiency further. XRD, FTIR, SEM-EDX, and BET were used to characterize the physicochemical characteristics of the corresponding catalysts. To optimize

catalyst preparation and transesterification conditions, results from CaO loading, calcination temperature, catalyst loading, oil to methanol molar ratio, and reaction period were thoroughly examined for the operation. Furthermore, the reusability of the catalyst was thoroughly researched. In addition, this study made a distinction between the prepared catalyst and other documented biochar-based catalysts.

2. Results and Discussions

2.1. Catalyst Characterization

2.1.1. XRD

XRD pattern peach shell biochar before and after activation along with modified activated carbon with CaO at 650 °C were presented in Figure 1.

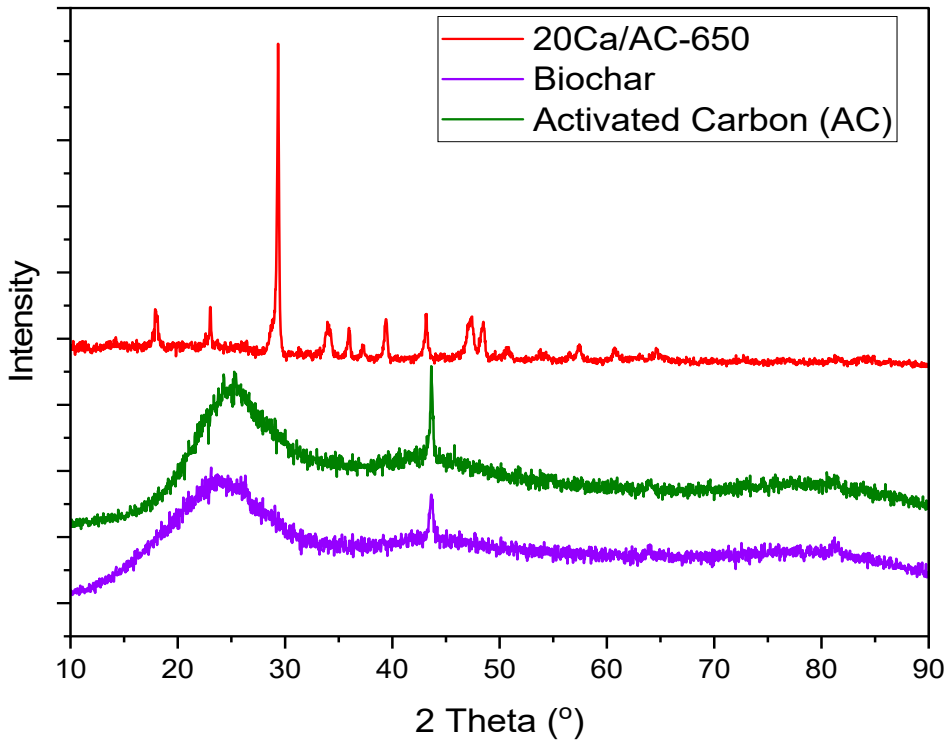

Figure 1. XRD patterns of Biochar, Activated Carbon, and 20Ca/AC-650.

Biochar and activated carbon samples showed a wide peak between 2θ = 10° and 30°), and a sharp stretching peak in the activated carbon sample at 2θ = 42°–45° ascribed to the presence of hexagonal graphitic carbon, indicating the synthesis of mesoporous structure. Afterwards, when activated carbon is loaded with CaO, clear diffraction peaks could be observed at 2θ = 32.2°, 37.35°, 53.80°, 64°, and 67.31°, demonstrating the existence of CaO crystallites and hence justifying Ca loading on active sites. The sharp peak at 2θ = 29.5° in the XRD sample of calcium-loaded activated carbon is due to the presence of $CaCO_3$, which is formed as a result of the reaction between loaded CaO and CO_2 during the synthesis process of catalyst [60,61].

2.1.2. Surface Area and Pore Volume Analysis

Table 1 outlines the physical characteristics of *Prunus persica* shell biochar specimens. The pure biochar sample, referred to as PB, has a BET surface area of 25.73 m^2/g and a pore volume of 61.36 mm^3/g. A substantial increase in surface area from 25.73 m^2/g to 281.90 m^2/g and pore volume from 61.36 mm^3/g to 297.07 mm^3/g was observed after activation by KOH. In addition, scanning electron microscopy (SEM) justified such modifications. The surface area and pore volume of activated biochar loaded with CaO were significantly reduced from 281.90 m^2/g to 64.95 m^2/g and 297.07 mm^3/g to 71.61 mm^3/g,

respectively. The decrease in pore volume was verified by the presence of CaO impregnated on pore channels, which indicated that the catalytic support surface had been coated by Ca compounds, hence blocking the apertures of the catalyst. The calcination temperature had a major impact on surface area and total pore volume. When the calcination temperature climbed from 500 to 600 °C, the surface area and pore volume of the 20Ca/AC catalyst increased from 62.38 to 64.95 m^2/g and from 64.82 to 71.61 mm^3/g, respectively. When the calcination temperature increases to 800 °C, however, the decomposition rate decreases dramatically; this might be because the calcination temperature was too excessive, leading to the sintering of the catalyst surface. Furthermore, the surface area and pore volume fell from 67.72 m^2/g and 86.14 mm^3/g to 55.87 m^2/g and 59.89 mm^3/g, respectively, when the CaO loading increased from 15 wt% to 30 wt%. As a result of the increased CaO, surface morphology may be affected.

Table 1. Sample properties.

Catalyst	Surface Area (m^2/g)	Pore Volume (mm^3/g)	Basic Strength (H_)	Total Basicity (mmol/g)
PB	25.73	61.36	7.2 < H_ < 9.8	1.5
AC	281.90	297.07	7.2 < H_ < 9.8	1.7
15Ca/AC-650	64.72	86.14	9.8 < H_ < 15.0	6.9
20Ca/AC-650	60.95	71.61	15.0 < H_ < 18.4	11.5
25Ca/AC-650	55.87	56.89	15.0 < H_ < 18.4	11.1
20Ca/AC-600	62.38	61.82	15.0 < H_ < 18.4	8.6
20Ca/AC-700	50.49	37.52	9.8 < H_ < 15.0	6.8

2.1.3. Basic Strength

Table 1 shows the distribution of strength and the overall basicity of the samples. According to the obtained results, biochar beforehand and after activation had strength values up to H_ < 9.8, and the total basicity values of both samples were 1.5 and 1.7 mmol/g, respectively. As CaO was added from 15% to 30%, the total basicity of the samples rose from 1.5 to 11.1 mmol/g, and the basic strength was in the range of 15.0 < H_ < 18.4. Additional CaO loading, on the other hand, reduced overall basicity. The maximum overall basicity of a 20 wt.% CaO-loaded catalyst was attributed to the presence of Ca compounds and totally decomposed CaO on the catalyst surface, which was worth mentioning. There was insufficient CaO and Ca compound phases with lesser CaO decomposition on the catalyst surface (15 wt.%). Nevertheless, with a CaO loading of more than 20 wt.%, the biochar phase could not be covered entirely by the CaO due to its excessive amount. XRD's prior findings were very much in line with these results. In addition, the temperature at which the catalyst is calcined has a role in its basicity. The sample's base strength and total basicity were H_ < 15.0 and 7.1 mmol/g, respectively, when the catalyst was calcined at 600 °C. At lower calcination temperatures, inactive phases could not completely break down, resulting in the poor basicity of this catalyst. At the 650 °C activation temperature, the total basicity was clearly enhanced (from 7.1 to 11.5 mmol/g) and finally reduced to 6.8 mmol/g at the calcination temperature of 700 °C, indicating that the activation temperature should not be increased further. According to data from the Surface area, catalyst surface area decreased mostly due to reduced basic sites (Table 1).

2.1.4. SEM and EDX

Figure 2 indicates that the surface structure of the catalysts examined by the SEM analyzer differs drastically. Figure 2a shows the biochar's SEM image which depicts low mesoporosity and rough structure, giving it a textured appearance. The emission of noxious compounds during heat treatment resulted in a shape that facilitates calcium ions' absorption and binding. Biochar treatment resulted in an uneven, porous surface, as seen in Figure 2b. Even this outcome was in line with the BET results of the treated biochar sample, which shows dramatically enhanced pore volume. Compared with the previous

findings, it was clear that CaO evenly covers the activated carbon support, resulting in a highly porous catalyst with even pore distribution on the catalyst's surface. As a result, we can see a dramatic increase in the basic strength and surface area of the synthesized calcium-coated activated carbon catalyst.

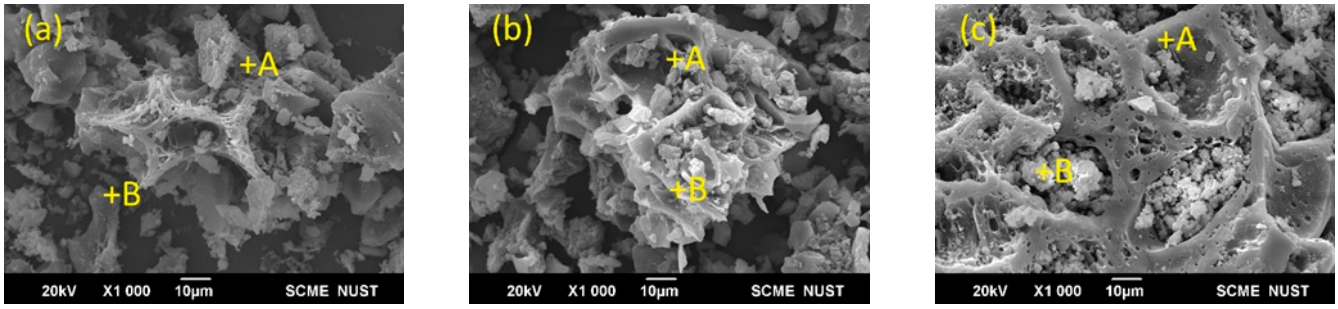

Figure 2. SEM images (**a**) peach shell biochar, (**b**) activated carbon and (**c**) 20Ca/AC-650.

Along with that, the EDX analysis is given in Table 2. C and O accounted for the bulk of the biochar, with a small quantity of Si and some metal components such as K, Mg, Al, and Ca making up the rest of the composition. C and O concentrations rose somewhat, whereas metal concentrations slightly reduced after KOH activation. According to the findings shown above, the activation of biochar might have increased the number of O-containing groups in the activated carbon samples. Ca was evenly deposited on the carbon support through the wet impregnation process. There are noticeable increases in the amount of calcium (Ca) content when 20 wt.% CaO is loaded onto the catalytic support. The calcium content of the finished catalyst ranged from 12.7 to 12.9 wt.%, indicating that the impregnated Ca was effectively deposited on the activated carbon catalyst support.

Table 2. EDX analysis (a) Biochar (b) Activated carbon and (c) 20Ca/AC-650.

Figures	Text Point	Elements Content (wt%)							
		C	O	Si	Al	Ca	Mg	K	Others
Figure 2a	A	81.2	12.4	2.1	1.2	0.7	0.9	0.8	0.7
	B	80.6	12.3	2.5	1.0	0.9	1.1	1.0	0.6
Figure 2b	A	83.0	13.8	0.7	0.5	0.3	0.7	0.6	0.4
	B	83.3	13.6	0.6	0.4	0.5	0.6	0.5	0.5
Figure 2c	A	67.3	16.6	0.7	0.5	12.9	0.8	0.5	0.7
	B	68.0	16.1	0.6	0.6	12.7	0.7	0.4	0.9

2.1.5. FTIR

With the aid of FTIR analysis, the structural knowledge of the prepared samples could be studied. Figure 3 depicts the FTIR data of biochar, and its activated sample and the final optimized catalyst utilized throughout our experimentation 20Ca/AC-650 catalyst. At 3450 cm^{-1} wideband could be observed in all characterized samples; this band was portraying the presence of the -OH group at the catalyst surface. When activated carbon is loaded with CaO, a sharp peak can be observed near 1470 cm^{-1}, 873 cm^{-1}, and 714 cm^{-1} correlated with asymmetric stretch showing the presence of CaCO3, which is mainly due to incomplete carbonization CaO. Literature studies revealed that $Ca(OH)_2$ structural hydroxyl groups are responsible for the abrupt extending band at 3644 cm^{-1} [62]. Aromatic hydrocarbon molecules were linked by C=C extending in the FTIR spectrum of biochar observed by the 1620 cm^{-1} band, and the C–O stretching of hydroxyl groups was linked by plan bands at 1120, 1088, and 1056 cm^{-1} [37]. These results were also justified by XRD patterns shown in Figure 3.

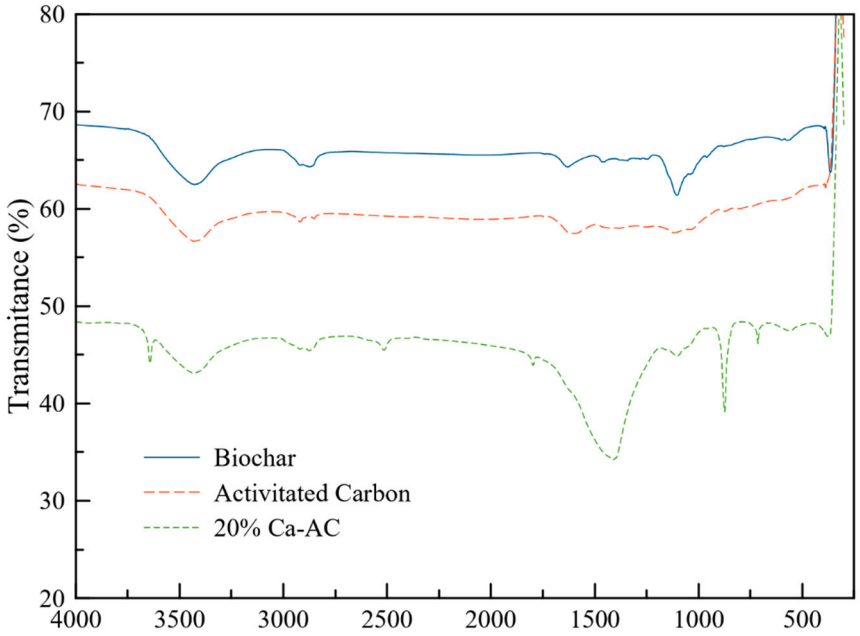

Figure 3. FTIR of Biochar, Activated carbon and 20Ca/AC-650 catalyst.

2.2. Catalyst Activity

Optimization of Reaction Conditions

The 20Ca/AC-650 catalyst that had been previously optimized was used in subsequent tests to discover the optimal reaction conditions. These experiments investigated the influence of several reaction parameters, such as reaction time, reaction temperature, oil to methanol molar ratio, and catalyst loading, on biodiesel production.

The FAME conversion of WCO as a function of the oil-to-methanol molar ratio is shown in Figure 4a. According to Lee Chateleir's principle, when a reversible reaction occurs, the balance moves towards the direction where stress may be released. Due to the fact that transesterification is a reversible process, a higher concentration of alcohol is required than that specified in the stoichiometric ratio (1:3). Surplus methanol causes stress on the reactant side, which reduces stress on the methyl ester side of the product and helps move the equilibrium of the reaction in the forward direction [63]. Biodiesel production was examined to be only 58% in a low oil to methanol molar ratio. Increasing the methanol concentration increased the reaction yield, which peaked at 1:8 and then had minimal effect on subsequent yields. Excess methanol dilutes the concentration of the product, resulting in lower biodiesel production; this finding showed that a 1:8 molar ratio was enough to achieve the highest possible catalytic efficiency.

This was followed by an optimization process for the determination of the ideal catalyst weight percentage for the transesterification of WCO shown in Figure 4b. For such heterogeneous catalyst-based reactions, the catalyst is the most crucial factor in determining whether the reaction will occur. Activated sites are only present in those catalyst areas that are directly exposed to the reactant solution. As a result, the total number of accessible active sites in a reaction can only be determined by the catalyst's concentration or weight percent; therefore, a higher catalyst concentration is regarded as introducing an increased number of active sites, which may strengthen the FAME conversion. WCO transesterification using 20Ca/AC-650 catalyst was speeded to the greatest extent in the presence of a catalyst concentration of 5 wt%, as shown in Figure 4b; this reaction, however, was hindered by fluid viscosity in the reaction medium if the catalyst weight was more than 5%. Viscous solutions severely disrupt mass transfer between reactants, products, and catalysts, as evidenced by an optimization plot reduction in FAME conversion at a high catalyst concentration.

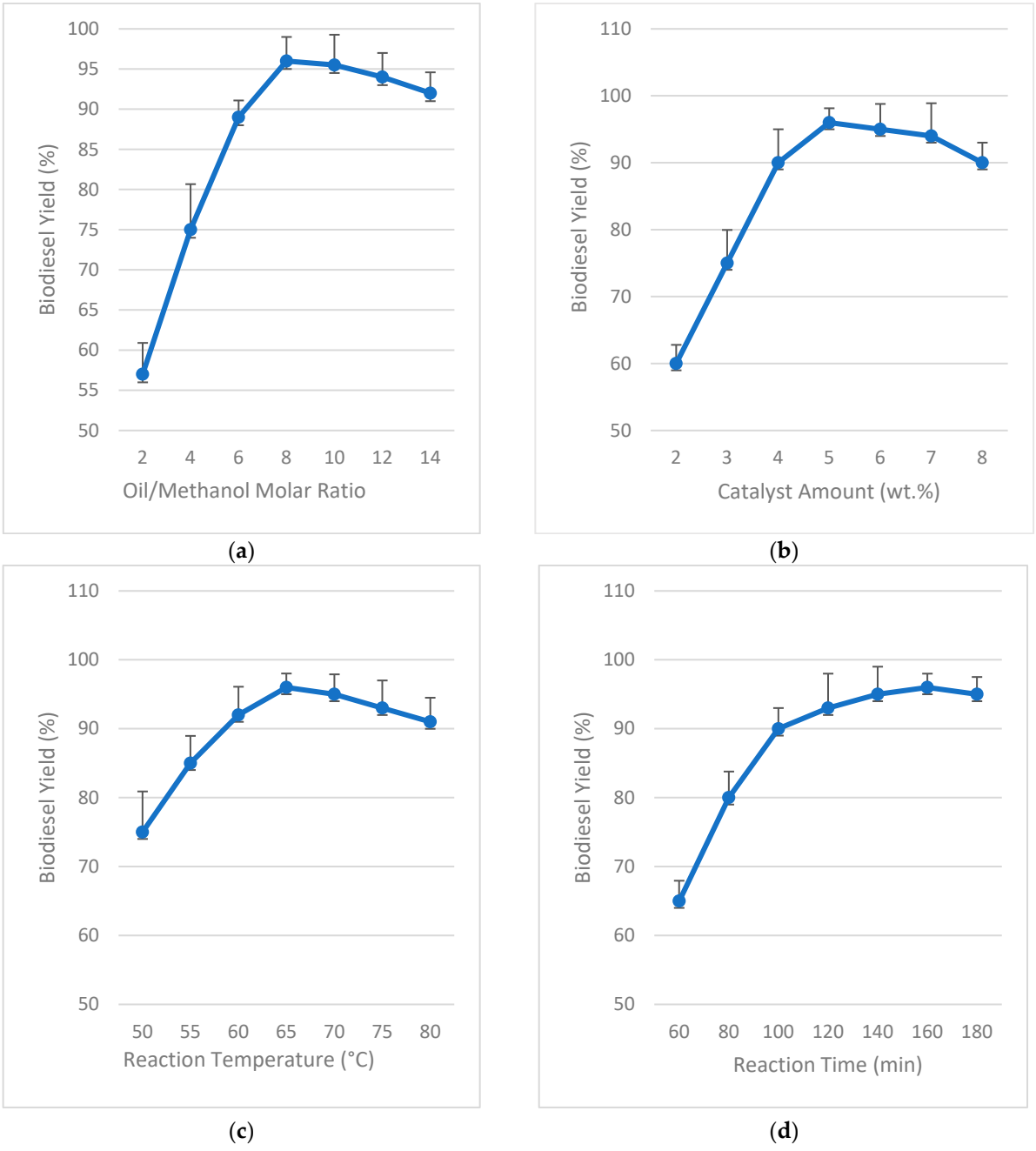

Figure 4. Influence of reaction conditions on the FAME yield on a 20Ca/AC-650 catalyst (all reactions carried out at optimum conditions, i.e., an oil-to-methanol molar ratio of 1:8, catalyst amount 5 wt.%, reaction temperature 65 °C, and reaction time 160 min) (**a**) Oil to methanol molar ratio, (**b**) Catalyst amount, (**c**) Reaction temperature and (**d**) Reaction time.

The kinetics of a chemical reaction is controlled by two major aspects such as reaction time and reaction temperature. By conducting a number of experiments at temperatures ranging from 50 °C to 80 °C, the effect of temperature on WCO's FAME production was determined. Throughout this temperature optimization process, the following parameters have been used: a molar ratio of 1:8, a catalyst weight of 5%, a temperature range of 50 °C to 80 °C with a 5 °C gap, and a time frame of 160 min. In Figure 4c, the results show that FAME production accelerated from 50 °C to 65 °C but decreased beyond 65 °C. Due to this, the temperature for this transesterification method was therefore set at 65 °C, which is close to the boiling point of methanol. Generating external energy to pass the

cutoff limit and initiate the reaction in a forward direction was only possible when the system reached its optimal operating conditions. At 65 °C, which is adjusted as optimal temperature, the acyl acceptor formed from methanol was found to be engaged entirely so that it could make FAME, or biodiesel, with the highest results. Unfortunately, at higher temperatures, methanol began to evaporate, causing a considerable loss of methanol. In other words, when the reaction temperature increased above its optimal level, the FAME conversion decreased.

Another critical constraint was adjusted by prolonging the duration of the process by 3 h under the following conditions: 1:8 oil to methanol molar ratio, 5 wt% catalyst concentration, 65 °C reaction temperature transesterification process. The response time, which varied from one hour to three hours, is shown in Figure 4d. Within just 100 min, the yield jumped from a low of 65% to a high of 90%. As the duration was further increased 160 min, the yield steadily rose to 96%. As a result, the ideal time of the process was set to 160 min; however, increasing the process duration beyond 160 min does not show an impact on enhancing yield. It is conjectured that FAME synthesis was subtracted beyond that optimal period due to stimulation of backward reactions, such as the breakdown of the methyl ester.

2.3. Reusability Test

By retrieving and reutilizing the catalyst in the transesterification process, we were able to examine the potential of sustainable heterogeneous and recyclable catalyst synthesis from the *Prunus persica* shell. To remove the oil from the catalyst surface, methanol and tetrahydrofuran were used to thoroughly wash it, followed by drying in a vacuum oven at 105 °C after it had been extracted from the reaction mixture. The catalytic performance of 20Ca/AC-650 was tested using the recycled catalyst in consecutive cycles under optimized conditions: reaction temperature 65 °C, reaction time 140 min, catalyst loading 5 wt%, and oil to methanol molar ratio 1:8. As shown in Figure 5, the 20Ca/AC-650 catalyst yield decreased from 96.0% to 81.50% over the first 10 cycles of the transesterification reaction. Reusability results revealed that the CaO-supported carbon-based catalyst is highly stable and sustainable even after 10 repeated cycles.

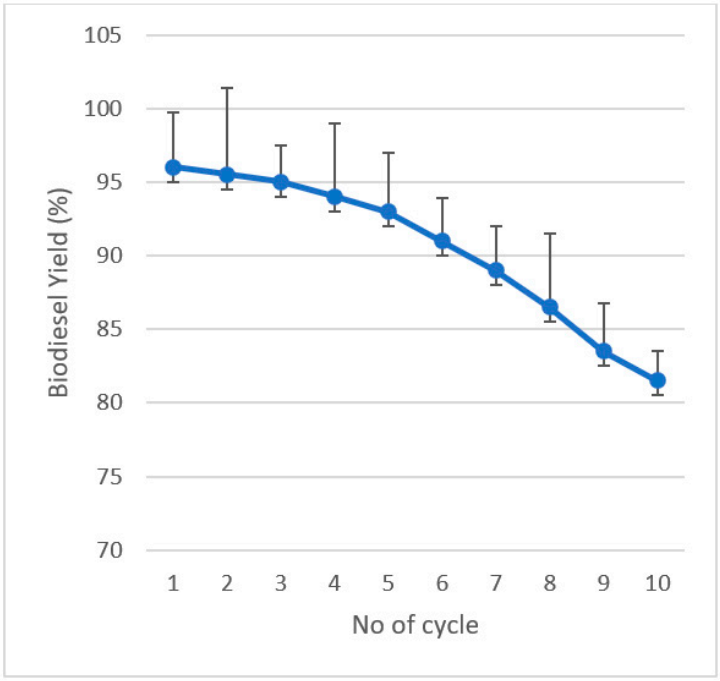

Figure 5. Reusability test of the 20Ca/AC-650 catalyst.

The XRD approach shown in Figure 6 was applied to investigate the depreciation of the catalyst in more detail for both fresh and spent 20Ca/AC-650 catalysts recovered after the 10th cycle. More substantial peaks of Ca in the XRD pattern of fresh 20Ca/AC-650 catalyst could be observed compared to the spent catalyst recovered after the 10th cycle, therefore showing weak calcium peaks; this result indicated the leaching of Ca^{+2} from the active site in every cycle, which ultimately led to a decrease in overall calcium content on the catalyst surface.

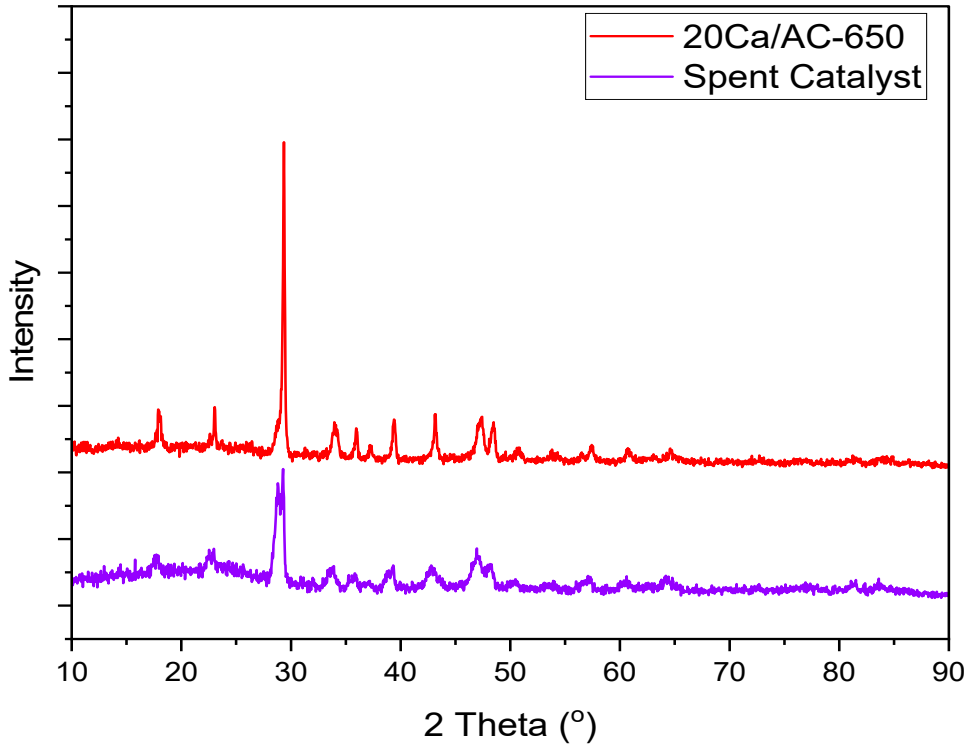

Figure 6. XRD of 20Ca/AC-650 and spent catalyst.

2.4. Biodiesel Characterization

2.4.1. Optimization of Catalyst Preparation Conditions

Figure 7 shows the impact of preparation conditions on the biodiesel yield of several catalysts. Figure 7a shows that when CaO loading increased from 10 to 20% by weight, the yield increased from 60% to 96%. BET studies showed that when CaO was added, the catalyst's catalytic activity dramatically increased because of its higher total basicity; however, biodiesel production had no discernible improvement when the CaO loading increased to 30%. In contrast to the surface area, the basicity was shown to have a larger impact on catalytic activity. Based on the foregoing data, it can be concluded that a CaO loading of less than 20% was insufficient for the transesterification process to proceed because of the lower number of basic sites available. Even with higher CaO loadings of more than 20 wt.%, the catalyst's catalytic performance was not significantly improved. It is possible that inadequate diffusion of the active species on the catalyst surface was caused by the crystallization or agglomeration of Ca compounds. Therefore, the catalyst with a CaO loading of 20 wt.% was selected for a further transesterification process.

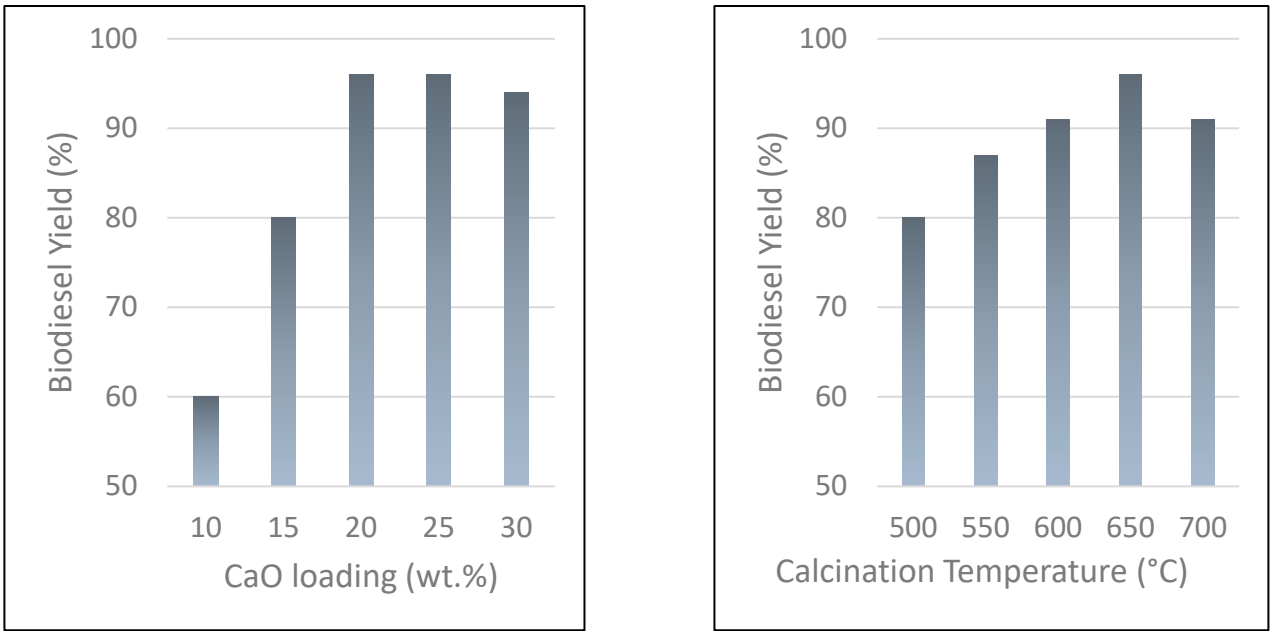

(**a**) (**b**)

Figure 7. Impact of catalyst preparation conditions on FAME yield (**a**) CaO loading and (**b**) Calcination temperature.

Figure 7b shows the influence of varying catalyst calcination temperatures on the conversion of WCO to FAME. Activated catalysts were tested for their ability to perform at the following reaction parameters: 500 °C, 550 °C, 600 °C, 650 °C, and 700 °C. 1:8 oil to methanol molar ratio, 5% catalyst weight, 65 °C reaction temperature, and 160 min reaction time. According to the findings of this research, increasing the catalyst activation temperature enhances catalytic efficiency. At 650 °C, the calcium oxide-loaded activated carbon-based catalyst had the maximum activity; however, as the calcination temperature continued to climb to 700 °C, there was a small drop in yield (from 96.0% to 91.0%). At increasing temperatures, the overall basicity of the solution decreases. The catalyst loading of 20% by weight CaO and a calcination temperature of 650 °C were the best values. Catalytic testing revealed that the 20Ca/AP-650 catalyst provided the best results for transesterification reactions. Based on the preceding descriptions of catalysts, it is also possible to deduce that the catalytic activity is mostly due to the basicity of the catalysts.

2.4.2. GC-MS

Figures 8–13 show the data obtained from the GC-MS analysis of biodiesel made from waste cooking oil. N-hexane (1.35%), 9-Hexadecanoic acid methyl ester (0.29%), Hexadecanoic acid methyl ester (16.17%), 9-Octadecanoic acid (Z)- methyl ester (61.69%), Methyl stearate (7.07%) and Bis(2-ethylhexyl) phthalate (13.43%) were the six primary fatty acids present in biodiesel.

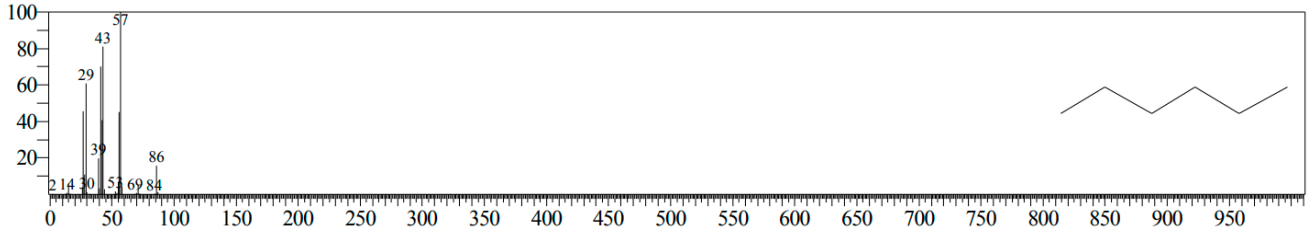

Figure 8. Comp Name: n-hexane, Run Time: 2.480, Mol Weight: 86.

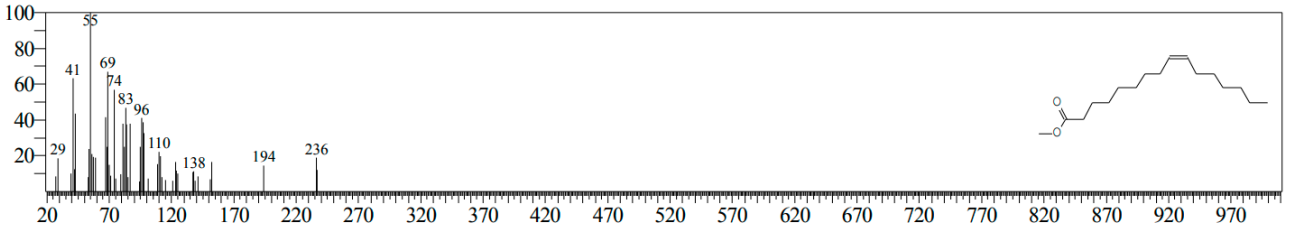

Figure 9. Comp Name: 9-Hexadecanoic acid, methyl ester, Run Time: 15.167, Mol Weight: 268.

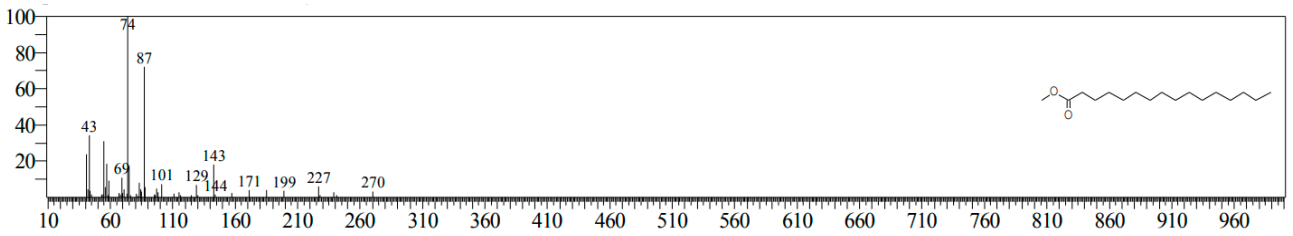

Figure 10. Comp Name: Hexadecanoic acid, methyl ester, Run Time: 15.402, Mol Weight: 270.

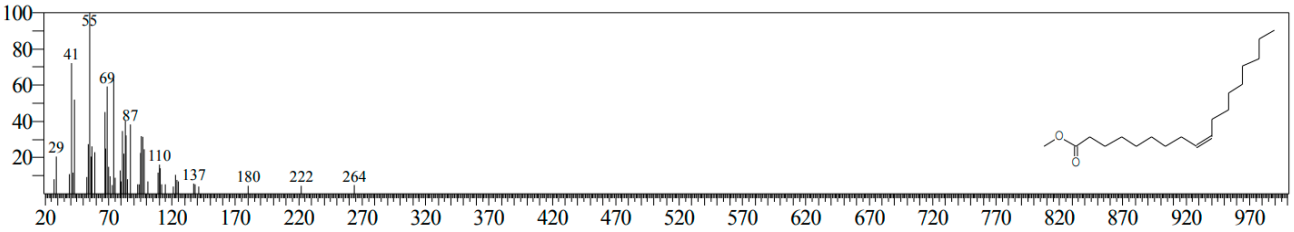

Figure 11. Comp Name: 9-Octadecanoic acid (Z)-, methyl ester, Run Time: 17.386, Mol Weight: 296.

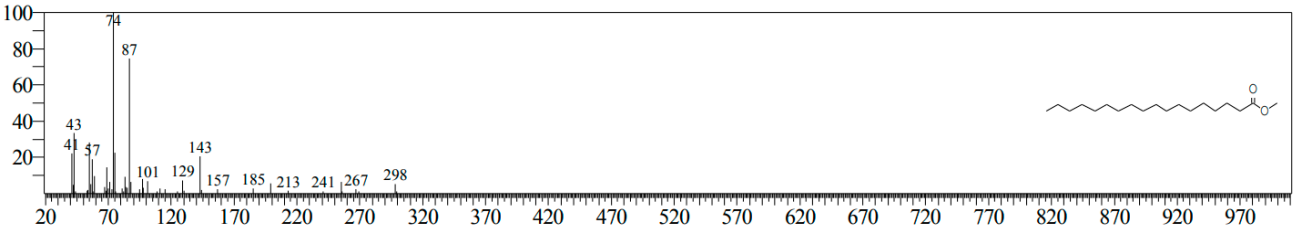

Figure 12. Comp Name: Methyl stearate, Run Time: 17.664, Mol Weight: 298.

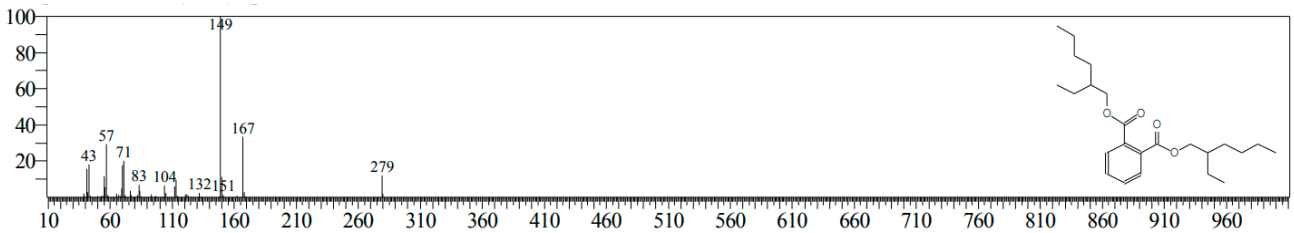

Figure 13. Comp Name: Bis(2-ethylhexyl) phthalate, Run Time: 21.973, Mol Weight: 390.

According to the research, the obtained biodiesel composition has 13.33% saturated FAME, 33.33% monounsaturated FAME, and 53.33% polyunsaturated FAME. Because of the increased degree of unsaturation in FAME constituents, biodiesel has strong combustible properties and high-power output [64,65]. Table 3 shows the obtained data from GC-MS along with the compositional proportions of fatty acids in biodiesel prepared from WCO.

Table 3. Compounds detected from GC-MS of biodiesel.

Retention Time	Fatty Acid Methyl Ester (FAME)	Composition (%)	Library Match	Corresponding Fame Formula
2.480	n-Hexane	1.35	98	C_6H_{14}
15.167	9-Hexadecanoic acid, methyl ester	0.29	99	$C_{17}H_{32}O_2Me$
15.402	Hexadecanoic acid, methyl ester	16.17	97	$C_{17}H_{34}O_2Me$
17.386	9-Octadecanoic acid (Z)-, methyl ester	61.69	98	$C_{19}H_{36}O_2Me$
17.664	Methyl stearate	7.07	98	$C_{19}H_{38}O_2$
21.973	Bis(2-ethylhexyl) phthalate	13.43	96	$C_{24}H_{38}O_4$
	Saturated FAME	13.33%		
	Monounsaturated FAME	33.33%		
	Polyunsaturated FAME	53.33%		

2.4.3. Physicochemical Characteristics of Prepared Biodiesel

The economic feasibility of biodiesel is strongly influenced by its fuel characteristics. Therefore, the physical and chemical properties of the biodiesel obtained, such as ester content, viscosity, moisture content, flash point, cetane number, acid number, density, and oxidation stability, were compared in Table 4 with the specifications ASTM D6751 and EN 14214. It was determined that all of the mentioned attributes were within the biodiesel standard tolerances set by ASTM D6751 and EN 14214. In other words, it guarantees that the biodiesel generated has a great potential to be a replacement fuel for petroleum distillate.

Table 4. Physicochemical Properties of Synthesized Biodiesel.

Properties	ASTM D6751	EN 14214	Biodiesel
Acid number (mg KOH/g)	≤0.5	<0.5	0.45
Viscosity (mm^2/s)	1.9–6.0	3.50–5.00	4.1
Cloud point (°C)	−3–12	-	3
Flash point (°C)	<130	<120	150
Pour point (°C)	−15–16	-	7
Cetane number	>47	>51	52
Density (kg/m^3)	860–894	860–900	887
Calorific value (MJ/kg)	35–42	-	41

2.5. Comparison of Catalytic Activity with Other Carbon-Based Catalysts

Table 5 illustrates the comparative study between the synthesized 20Ca/AC-650 catalyst and the carbon-based catalysts that have been previously reported in the literature for the transesterification process. The assembled data proved that the newly synthesized catalyst exhibits catalytic activity similar to other carbon-based catalysts that have been previously reported, showing that the 20Ca/AC-650 catalyst was an effective catalyst for the transesterification process and showed considerable potential for industrial use.

Table 5. Comparison of the catalytic performance of 20Ca/AC-650 and other carbon-based catalysts.

Catalyst	Support	Reaction Conditions				Biodiesel Yield (%)	Ref.
		Catalyst Loading (wt.%)	Temp. (°C)	Time (min)	Molar Ratio		
$CaO/K_2CO_3/BC$	Algal biochar	4	65	200	18	98.83	[66]
K_2CO_3/BC	Pomelo peel biochar	6	65	150	8	98	[35]
PPBC	Potato peel biochar	3	60	120	9	97.5	[67]
CaO/SiO_2	Peat biochar	5	65	150	8	93.4	[37]
CaO/SiO_2	Rice husk biochar	8	65	180	9	93.4	[36]
$KOH/Ca(NO_3)_2$	Coconut endocarp activated carbon	10	60	480	15	90.8	[68]
SrO-Carbon	Date seed activated carbon	4	65	90	15	94.27	[69]
CaO/AC	*Prunus persica* shell activated carbon	5	65	140	8	96	Present work

3. Materials and Methods

3.1. Materials

The shells of peaches (*Prunus persica*) were collected in summer from the local fields of Swat (Pakistan). Waste chicken eggshells and waste cooking oil were collected from the student cafeteria of the NUST H-12 Islamabad campus. Some significant physicochemical features of the waste cooking oil were explored before it was used in transesterification, as illustrated in Table 6. All other chemicals used in this research, such as analytical grade methanol (99.5%), potassium hydroxide (99%), and tetrahydrofuran (99.8%), were purchased from Sigma-Aldrich Chemical Co. Ltd (St. Louis, MO, USA). All of the chemicals are acquired with the maximum purity and utilized without any further purification. Throughout the process, deionized water was used.

Table 6. Physicochemical properties of waste cooking oil (WCO).

Properties	Waste Cooking Oil	ASTM Standard Method
Acid Value (mg KOH/g oil)	1.62	D664
Saponification number (mg KOH/g oil)	205.3	D9407
Iodine number (mg I2/g)	133.9	D2500
Calorific value (MJ/kg)	38.4	D240
Viscosity (mm^2/s) at 40 °C	68.6	D7110
Density (kg/m^3) at 27 °C	906	D4052
Refractive Index	1.50	D1717
pH	5.7	-

3.2. Biochar Preparation and Activation

The collected *Prunus persica* shells were washed with deionized water to remove impurities and dust, followed by overnight drying at 100 °C. After being dried, the *Prunus persica* shells were finely grounded to pass the mesh size 0.250 mm screen using a vibratory sieve shaker. The *Prunus persica* biochar was then prepared at 650 °C and kept in a vertical furnace for 2 h in an N_2 environment. The schematic representation of the *Prunus persica* shell in biochar is shown in Figure 14. The biochar obtained was chemically activated by KOH treatment. In general, 2 g of *Prunus persica* biochar was mixed and stirred for 3 h with a solution of 500 mL of 2 M KOH. The suspension's biochar extraction was performed using VWR Qualitative Filter Paper (Model 28,321-077). The biochar retained on the filter paper was then washed with deionized water until neutral pH of the filtrate was attained. The biochar collected was eventually kept at 105 °C in an oven for drying. The activated samples of prepared peach shell biochar (*Prunus persica*), later referred to as AC (activated carbon), were contained in an airtight container.

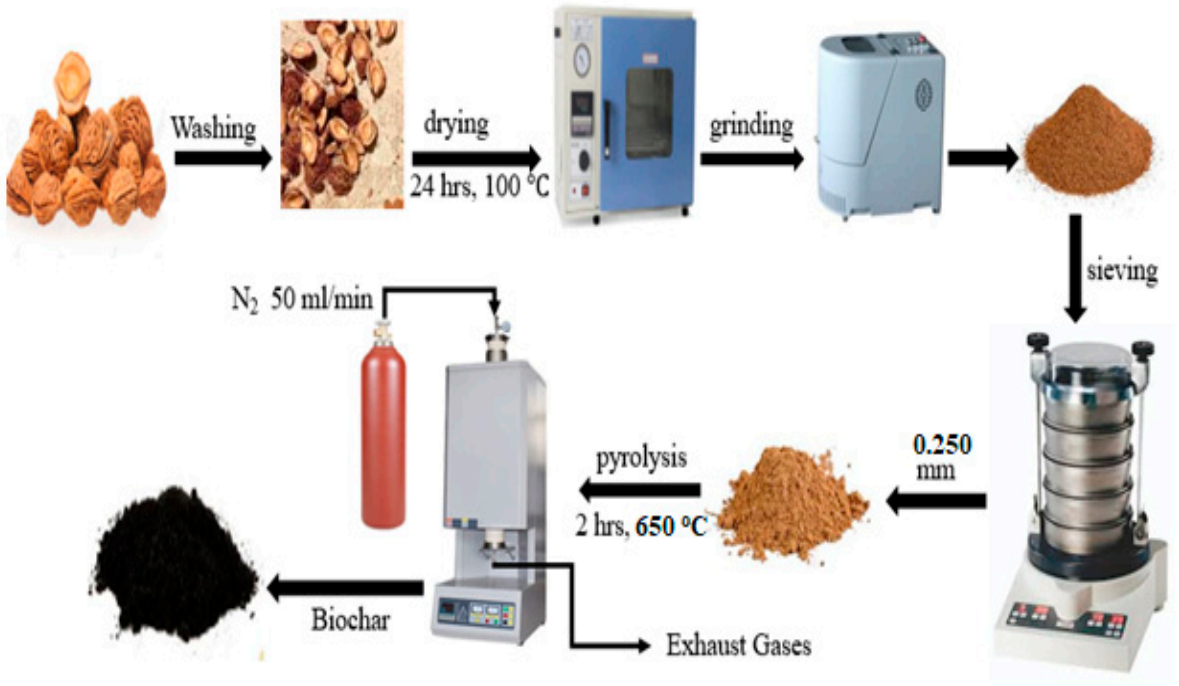

Figure 14. Schematic diagram of biochar preparation.

3.3. Eggshell Calcium Oxide Preparation

Originally, the waste chicken eggshells were collected from NUST Cafe and cleaned many times with deionized water to eliminate any impurities present. It was then dried for 24 h in an oven at 100 °C. The shell was then ground to powder using a grinder to slip through a 0.250 mm sieve. The powdered shell was eventually calcinated in a muffle furnace for 3 h at a temperature of 900 °C. The CaO obtained was then soaked in water for 6 h at 60 °C, followed by overnight drying in an oven at 120 °C. The material was finally dehydrated to convert hydroxide to oxide at 600 °C for 3 h by calcination and stored for future use in a desiccator. Calcined eggshells provide very active CaO. Figure 15 shows the schematic diagram for the conversion of chicken eggshells waste into CaO.

Figure 15. Schematic diagram of CaO synthesis.

3.4. Catalyst Preparation

A wet impregnation process was used to prepare a CaO-promoted AC catalyst. The AC was mixed with CaO-impregnating solution, which was formulated at different concentrations (10 wt%, 15 wt%, 20 wt%, 25 wt%, and 30 wt%). According to the standard method [35], 2.0 g of powdered CaO was gradually mixed with 100 mL of deionized water to prepare a 20 wt% CaO loaded catalyst, accompanied by the addition of 8.0 g of dried AC, followed by stirring at 800 rpm for 1 h. The suspension was then dried for 24 h at 105 °C, accompanied by activation at 500–700 °C for 3 h. The prepared catalysts were referred to as αCa/AC-T; here, α and T outline the CaO loading (wt%) and the activation temperature, respectively.

3.5. Catalyst Characterization

In an attempt to analyze the surface morphology of the samples, the scanning electron microscopy (SEM) study was performed. In addition, energy-dispersive X-ray spectroscopy has been used to track the high-resolution surface morphology of the samples. Both techniques were performed on TESCAN VEGA 3 (Tescan Analytics, Brno, Czech Republic), operated by a secondary electron detector and a tungsten detector with a high voltage of 20 kV at an angle of 45 °C. To gain more insight into anatomy, the SEM images were obtained in three distinct sizes of 4, 6, and 8 μm.

The Cary 630 FTIR model spectrometer from Agilent Technologies (Santa Clara, CA, USA) was used to investigate the creation of new bonds and the dissolution of existing ones. The wavelength of the apparatus was adjusted at 650–4000 cm^{-1} for scanning the samples of the prepared catalyst. The specimen was diffused using a reflectance process through the ZnSe diffuse reflective accessory (DRA).

XRD analysis was performed using the Bruker XRD (D8 Advance) (Hamburg, Germany), fitted with ni-filtered Cu Kα (C = 0.15418 nm) radiations, to study the crystalline, semicrystalline, or amorphous composition. Samples were scanned using a scanning rate of 0.05 °C min^{-1}. JADE 6.0 was used to analyze the XRD patterns, and through the built-in option of JCPDS (Joint Committee on Powder Diffraction Standards) software repository, the peaks were recognized.

The Quantachrome NOVA 2200e (Boynton Beach, FL, USA) analyzer has been used for surface area analysis, at a temperature of −196 °C, of a nitrogen adsorption-desorption isotherm. A Brunauer–Emmett–Teller equation (BET) was used in the relative pressure of (0.05–0.25 kPa) to measure the surface area. In the relative pressure of 0.997 KPa, the average pore volume (Absolute) was estimated to be the sum of N_2 adsorption. The samples were degassed at 150 °C for 5 h until adsorption tests and estimates were performed for each sample individually. The values were observed to be within the range of ±2%.

The Hammett indicator method was used to assess the strength of the base. Anhydrous methanol solution (0.02 M) titration with Hammett indicator-benzene carboxylic acid was used to determine the catalysts' overall basicity.

3.6. Biodiesel Characterization

To determine the organic content of the FAME mixture, Gas Chromatography-Mass-Spectroscopy (GC-MS) is a strong analysis tool. The components in fatty acid methyl esters of waste cooking oil were evaluated using GC-MS. A Shimadzu SH-Rxi-5Sil mass spectrometer (Shimadzu, Tokyo, Japan) with column specifications of 30 m × 0.25 mm dimensions and a 0.25 m film thickness were used to examine feedstock composition. A flow rate of 1.5 mL/min of n-hexane was employed as the carrier gas through an auto-injector at 220 °C, and the split-less mode was activated. For an initial 1 min, the oven temperature was maintained at 80°C, and afterwards, it was gradually increased to 200 °C at a pace of 10°C/min. After that, the temperature was raised to 270 °C at a rate of 8 °C/min and kept there for another one min. To determine fatty acid methyl esters in produced waste cooking oil biodiesel samples, the resulting data were compared to the NIST database library.

3.7. Experimental Setup for the Parametric Study of the Biodiesel Production Process

Processes such as transesterification, separation, purification, and drying occur during the whole stage of biodiesel development. End products are glycerol and biodiesel. Glycerol has not been regarded as waste from finished processing due to its commercial importance, because glycerol may be used to make soap. The transesterification reaction of peach seed oil (*Prunus persica*) is carried out in a three-neck round bottom flask attached with a condenser, a thermometer, and a heating metal using CaO promoted peach shell (*Prunus persica*) activated carbon and methanol at atmospheric pressure. The reaction carried out in the reactor is represented as:

$$\text{Triglyceride} + \text{Methanol} \leftrightarrow \text{Methyl Esters} + \text{Glycerol}$$

The flask was kept at 65 °C for 140 min using a 1:8 oil to methanol molar ratio and a catalyst loading of 5 wt%. The catalyst was separated from the blend by centrifugation after the experiment was finished, where the filtrate was kept overnight in a separation funnel. To extract surplus methanol, a rotary evaporator was used under minimized pressure, and the excess methanol was separated. Finally, gas chromatography was used to examine samples of prepared biodiesel.

The following Equation (1) is used for the calculation of biodiesel *yield* [69].

$$Yield\ (\%) = \frac{weight\ of\ biodiesel \times\ \%\ FAME}{weight\ of\ oil} \times 100\% \quad (1)$$

where % *FAME* relates to *FAME* amounts (fatty acid methyl ester) derived through GC processing.

3.8. Catalyst Reusability

After the transesterification reaction, the catalyst was separated and recovered from biodiesel to determine its reusability. Then the spent catalyst was vigorously flushed with methanol and then tetrahydrofuran to remove the traces. Subsequently, it was kept at 105 °C for the removal of moisture and drying in an oven. Finally, the catalyst was reused directly for the next cycle.

4. Conclusions

This study has presented the liquid and solid waste management of waste cooking oil and residual fruit shells by conversion to biodiesel using a novel catalyst that inspires waste to fuel production; this was conducted via a solid base-catalyzed transesterification process. A cost-effective and novel peach shell-derived AC-supported CaO catalyst at 650 °C calcination temperature and 20% CaO loading has been designed. Following this, several characterization methods were used to examine the physical and chemical characteristics of the catalyst. At a 1:8 oil to methanol molar ratio, a catalyst weight of 5 wt%, a temperature of 65 °C and a duration of 160 min, the highest conversion rate, that is, 96% was achieved using 20Ca/AC-650. Furthermore, the recycling experiments showed that after being reused for 10 cycles, the catalyst maintained a high degree of stability above 80%. Ca^{2+} ions leaching into products was revealed to be the primary cause of a little deactivation of the catalyst. Several significant physical and chemical parameters of the synthesized biodiesel were then tested and confirmed to be within the permitted limit set by the ASTM D6751 standard. Petrodiesel may therefore be replaced by product biodiesel in CI engines that use a similar engine configuration. After all, has been said and done, it has been determined that 20Ca/AC-650 is a cost-effective, recyclable, sustainable recyclable, and seeping-proof catalyst for the production of faster and higher quality biodiesel. Furthermore, the environmental issues caused by WCO are intelligently resolved by converting it into biodiesel, which can eventually contribute to improving the country's economic situation.

Author Contributions: Conceptualization, A.H. and S.R.N.; methodology, A.H.; validation, S.R.N.; formal analysis, U.S.; investigation, U.S.; resources, S.R.N.; writing—original draft preparation, A.H. and W.-H.C.; writing—review and editing, A.H. and W.-H.C.; visualization, S.R.N.; supervision, S.R.N.; project administration, W.-H.C.; funding acquisition, All authors have read and agreed to the published version of the manuscript.

Funding: This research was funded by the National University of Sciences & Technology, Pakistan. The authors also acknowledge financial support from the Ministry of Science and Technology, Taiwan, R.O.C., under the grant numbers MOST 109-2221-E-006-040-MY3, MOST 110-2622-E-006-001-CC1, and MOST 110-3116-F-006-003-. This research is also supported in part by Higher Education Sprout Project, Ministry of Education to the Headquarters of University Advancement at National Cheng Kung University (NCKU).

Data Availability Statement: Not applicable.

Conflicts of Interest: The authors declare no conflict of interest. The funders had no role in the design of the study; in the collection, analyses, or interpretation of data; in the writing of the manuscript, or in the decision to publish the results.

References

1. Woodford, J.J.; Dacquin, J.P.; Wilson, K.; Lee, A.F. Better by design: Nanoengineered macroporous hydrotalcites for enhanced catalytic biodiesel production. *Energy Environ. Sci.* **2012**, *5*, 6145–6150. [CrossRef]
2. Gardy, J.; Hassanpour, A.; Lai, X.; Ahmed, M.H.; Rehan, M. Biodiesel production from used cooking oil using a novel surface functionalised TiO_2 nano-catalyst. *Appl. Catal. B Environ.* **2017**, *207*, 297–310. [CrossRef]
3. Naqvi, S.R.; Bibi, A.; Naqvi, M.; Noor, T.; Nizami, A.S.; Rehan, M.; Ayoub, M. New trends in improving gasoline quality and octane through naphtha isomerization: A short review. *Appl. Petrochem. Res.* **2018**, *8*, 131–139. [CrossRef]
4. Hardy, J.T. *Climate Change: Causes, Effects, and Solutions*; John Wiley & Sons: New York, NY, USA, 2003.
5. Naqvi, S.R.; Uemura, Y.; Yusup, S.; Sugiura, Y.; Nishiyama, N. In situ catalytic fast pyrolysis of paddy husk pyrolysis vapors over MCM-22 and ITQ-2 zeolites. *J. Anal. Appl. Pyrolysis* **2015**, *114*, 32–39. [CrossRef]
6. Correa, D.F.; Beyer, H.L.; Possingham, H.P.; Thomas-Hall, S.R.; Schenk, P.M. Biodiversity impacts of bioenergy production: Microalgae vs. first generation biofuels. *Renew. Sustain. Energy Rev.* **2017**, *74*, 1131–1146. [CrossRef]
7. Azeem, B.; KuShaari, K.; Naqvi, M.; Kok Keong, L.; Almesfer, M.K.; Al-Qodah, Z.; Naqvi, S.R.; Elboughdiri, N. Production and characterization of controlled release urea using biopolymer and geopolymer as coating materials. *Polymers* **2020**, *12*, 400. [CrossRef]
8. Gómez, A.; Rodrigues, M.; Montañés, C.; Dopazo, C.; Fueyo, N. The technical potential of first-generation biofuels obtained from energy crops in Spain. *Biomass Bioenergy* **2011**, *35*, 2143–2155. [CrossRef]
9. Naqvi, M.; Yan, J.; Dahlquist, E.; Naqvi, S.R. Waste biomass gasification based off-grid electricity generation: A case study in Pakistan. *Energy Procedia* **2016**, *103*, 406–412. [CrossRef]
10. Corro, G.; Pal, U.; Tellez, N. Biodiesel production from Jatropha curcas crude oil using ZnO/SiO_2 photocatalyst for free fatty acids esterification. *Appl. Catal. B Environ.* **2013**, *129*, 39–47. [CrossRef]
11. Li, M.; Zheng, Y.; Chen, Y.; Zhu, X. Biodiesel production from waste cooking oil using a heterogeneous catalyst from pyrolyzed rice husk. *Bioresour. Technol.* **2014**, *154*, 345–348. [CrossRef]
12. Pham, L.K.; Kongparakul, S.; Reubroycharoen, P.; Karnjanakom, S.; Naqvi, S.R.; Guan, G.; Samart, C. Biofuel production with integrated pyrolysis and catalytic upgrading system. In *Innovations in Thermochemical Technologies for Biofuel Processing*; Elsevier: Amsterdam, The Netherlands, 2022; pp. 147–177.
13. Sajjadi, B.; Raman, A.A.A.; Arandiyan, H. A comprehensive review on properties of edible and non-edible vegetable oil-based biodiesel: Composition, specifications and prediction models. *Renew. Sustain. Energy Rev.* **2016**, *63*, 62–92. [CrossRef]
14. Fadhil, A.B. Evaluation of apricot (*Prunus armeniaca* L.) seed kernel as a potential feedstock for the production of liquid bio-fuels and activated carbons. *Energy Convers. Manag.* **2017**, *133*, 307–317. [CrossRef]
15. Fadhil, A.B.; Alhayali, M.A.; Saeed, L.I. Date (*Phoenix dactylifera* L.) palm stones as a potential new feedstock for liquid bio-fuels production. *Fuel* **2017**, *210*, 165–176. [CrossRef]
16. Nehdi, I.A.; Sbihi, H.M.; Al-Resayes, S.I. Rhazya stricta Decne seed oil as an alternative, non-conventional feedstock for biodiesel production. *Energy Convers. Manag.* **2014**, *81*, 400–406. [CrossRef]
17. Inayat, M.; Shahbaz, M.; Naqvi, S.R.; Sulaiman, S.A. Advance strategies for tar elimination from biomass gasification techniques. In *Bioenergy Resources and Technologies*; Elsevier: Amsterdam, The Netherlands, 2021; pp. 61–88.
18. Abdullah, S.H.Y.S.; Hanapi, N.H.M.; Azid, A.; Umar, R.; Juahir, H.; Khatoon, H.; Endut, A. A review of biomass-derived heterogeneous catalyst for a sustainable biodiesel production. *Renew. Sustain. Energy Rev.* **2017**, *70*, 1040–1051. [CrossRef]
19. Bibi, I.; Shahid, M.; Niazi, N.K.; Younas, F.; Naqvi, S.R.; Shaheen, S.M.; Imran, M.; Wang, H.; Hussaini, K.M.; Zhang, H.J.; et al. Hydrogeochemical and health risk evaluation of arsenic in shallow and deep aquifers along the different floodplains of Punjab, Pakistan. *J. Hazard. Mater.* **2021**, *402*, 124074.

20. Lee, A.F.; Bennett, J.A.; Manayil, J.C.; Wilson, K. Heterogeneous catalysis for sustainable biodiesel production via esterification and transesterification. *Chem. Soc. Rev.* **2014**, *43*, 7887–7916. [CrossRef]
21. Khan, M.; Mehran, M.T.; Haq, Z.U.; Ullah, Z.; Naqvi, S.R.; Ihsan, M.; Abbass, H. Applications of artificial intelligence in COVID-19 pandemic: A comprehensive review. *Expert Syst. Appl.* **2021**, *185*, 115695. [CrossRef]
22. Uprety, B.K.; Chaiwong, W.; Ewelike, C.; Rakshit, S.K. Biodiesel production using heterogeneous catalysts including wood ash and the importance of enhancing byproduct glycerol purity. *Energy Convers. Manag.* **2016**, *115*, 191–199. [CrossRef]
23. Leung, D.Y.C.; Wu, X.; Leung, M.K.H. A review on biodiesel production using catalyzed transesterification. *Appl. Energy* **2010**, *87*, 1083–1095. [CrossRef]
24. Bajaj, A.; Lohan, P.; Jha, P.N.; Mehrotra, R. Biodiesel production through lipase catalyzed transesterification: An overview. *J. Mol. Catal. B Enzym.* **2010**, *62*, 9–14.
25. Semwal, S.; Arora, A.K.; Badoni, R.P.; Tuli, D.K. Biodiesel production using heterogeneous catalysts. *Bioresour. Technol.* **2011**, *102*, 2151–2161. [CrossRef] [PubMed]
26. Chen, L.; Zhang, F.; Li, G.; Li, X. Effect of Zn/Al ratio of Ni/ZnO-Al_2O_3 catalysts on the catalytic deoxygenation of oleic acid into alkane. *Appl. Catal. A Gen.* **2017**, *529*, 175–184.
27. Hameed, Z.; Naqvi, S.R.; Naqvi, M.; Ali, I.; Taqvi, S.A.A.; Gao, N.; Hussain, S.A.; Hussain, S. A comprehensive review on thermal coconversion of biomass, sludge, coal, and their blends using thermogravimetric analysis. *J. Chem.* **2020**, *2020*, 5024369. [CrossRef]
28. Chen, J.; Wang, C.; Pan, Y.; Farzana, S.S.; Tam, N.F.-Y. Biochar accelerates microbial reductive debromination of 2, 2′, 4, 4′-tetrabromodiphenyl ether (BDE-47) in anaerobic mangrove sediments. *J. Hazard. Mater.* **2018**, *341*, 177–186. [CrossRef] [PubMed]
29. Huang, H.-j.; Yang, T.; Lai, F.-y.; Wu, G.-q. Co-pyrolysis of sewage sludge and sawdust/rice straw for the production of biochar. *J. Anal. Appl. Pyrolysis* **2017**, *125*, 61–68.
30. Li, M.; Tang, Y.; Ren, N.; Zhang, Z.; Cao, Y. Effect of mineral constituents on temperature-dependent structural characterization of carbon fractions in sewage sludge-derived biochar. *J. Clean. Prod.* **2018**, *172*, 3342–3350. [CrossRef]
31. Ubando, A.T.; Chen, W.H.; Tan, R.R.; Naqvi, S.R. Optimal integration of a biomass-based polygeneration system in an iron production plant for negative carbon emissions. *Int. J. Energy Res.* **2020**, *44*, 9350–9366. [CrossRef]
32. Kostić, M.D.; Bazargan, A.; Stamenković, O.S.; Veljković, V.B.; McKay, G. Optimization and kinetics of sunflower oil methanolysis catalyzed by calcium oxide-based catalyst derived from palm kernel shell biochar. *Fuel* **2016**, *163*, 304–313. [CrossRef]
33. Lee, J.; Kim, K.-H.; Kwon, E.E. Biochar as a catalyst. *Renew. Sustain. Energy Rev.* **2017**, *77*, 70–79.
34. Naqvi, S.R.; Uemura, Y.; Osman, N.; Yusup, S. Production and evaluation of physicochemical characteristics of paddy husk bio-char for its C sequestration applications. *BioEnergy Res.* **2015**, *8*, 1800–1809.
35. Zhao, C.; Lv, P.; Yang, L.; Xing, S.; Luo, W.; Wang, Z. Biodiesel synthesis over biochar-based catalyst from biomass waste pomelo peel. *Energy Convers. Manag.* **2018**, *160*, 477–485.
36. Zhao, C.; Yang, L.; Xing, S.; Luo, W.; Wang, Z.; Lv, P. Biodiesel production by a highly effective renewable catalyst from pyrolytic rice husk. *J. Clean. Prod.* **2018**, *199*, 772–780. [CrossRef]
37. Wang, S.; Shan, R.; Wang, Y.; Lu, L.; Yuan, H. Synthesis of calcium materials in biochar matrix as a highly stable catalyst for biodiesel production. *Renew. Energy* **2019**, *130*, 41–49.
38. Chellappan, S.; Nair, V.; Sajith, V.; Aparna, K. Experimental validation of biochar based green Bronsted acid catalysts for simultaneous esterification and transesterification in biodiesel production. *Bioresour. Technol. Rep.* **2018**, *2*, 38–44.
39. Shan, R.; Zhao, C.; Lv, P.; Yuan, H.; Yao, J. Catalytic applications of calcium rich waste materials for biodiesel: Current state and perspectives. *Energy Convers. Manag.* **2016**, *127*, 273–283.
40. Bennett, J.A.; Wilson, K.; Lee, A.F. Catalytic applications of waste derived materials. *J. Mater. Chem. A* **2016**, *4*, 3617–3637.
41. Cho, Y.B.; Seo, G. High activity of acid-treated quail eggshell catalysts in the transesterification of palm oil with methanol. *Bioresour. Technol.* **2010**, *101*, 8515–8519.
42. Wilson, K.; Hardacre, C.; Lee, A.F.; Montero, J.M.; Shellard, L. The application of calcined natural dolomitic rock as a solid base catalyst in triglyceride transesterification for biodiesel synthesis. *Green Chem.* **2008**, *10*, 654–659. [CrossRef]
43. Ali, I.; Tariq, R.; Naqvi, S.R.; Khoja, A.H.; Mehran, M.T.; Naqvi, M.; Gao, N. Kinetic and thermodynamic analyses of dried oily sludge pyrolysis. *J. Energy Inst.* **2021**, *95*, 30–40.
44. Kouzu, M.; Kasuno, T.; Tajika, M.; Sugimoto, Y.; Yamanaka, S.; Hidaka, J. Calcium oxide as a solid base catalyst for transesterification of soybean oil and its application to biodiesel production. *Fuel* **2008**, *87*, 2798–2806. [CrossRef]
45. Li, H.; Niu, S.; Lu, C.; Li, J. Calcium oxide functionalized with strontium as heterogeneous transesterification catalyst for biodiesel production. *Fuel* **2016**, *176*, 63–71. [CrossRef]
46. Fan, M.; Liu, Y.; Zhang, P.; Jiang, P. Blocky shapes Ca-Mg mixed oxides as a water-resistant catalyst for effective synthesis of biodiesel by transesterification. *Fuel Processing Technol.* **2016**, *149*, 163–168. [CrossRef]
47. Boey, P.-L.; Maniam, G.P.; Hamid, S.A. Biodiesel production via transesterification of palm olein using waste mud crab (scylla serrata) shell as a heterogeneous catalyst. *Bioresour. Technol.* **2009**, *100*, 6362–6368. [CrossRef]
48. Nakatani, N.; Takamori, H.; Takeda, K.; Sakugawa, H. Transesterification of soybean oil using combusted oyster shell waste as a catalyst. *Bioresour. Technol.* **2009**, *100*, 1510–1513. [CrossRef]
49. Kouzu, M.; Kajita, A.; Fujimori, A. Catalytic activity of calcined scallop shell for rapeseed oil transesterification to produce biodiesel. *Fuel* **2016**, *182*, 220–226. [CrossRef]

50. Wei, Z.; Xu, C.; Li, B. Application of waste eggshell as low-cost solid catalyst for biodiesel production. *Bioresour. Technol.* **2009**, *100*, 2883–2885. [CrossRef]
51. Ullah, A.; Khan, D.; Zheng, S. The determinants of technical efficiency of peach growers: Evidence from khyber pakhtunkhwa, pakistan. *Custos E Agronegocio* **2017**, *13*, 211–238.
52. Ali, A.; Abdulai, A.; Goetz, R. Impacts of tenancy arrangements on investment and efficiency: Evidence from Pakistan. *Agric. Econ.* **2012**, *43*, 85–97. [CrossRef]
53. Imran, I.; Amanullah, D.R. Integration of peach (*Prunus persica* L.) biochar, compost and peach residues along with beneficial microbes and phosphorus improve agronomic efficiency, phosphorus use efficiency, partial factor productivity and soil p in soybean vs maize crops. *Preprints* **2019**. [CrossRef]
54. Lukić, I.; Krstić, J.; Jovanović, D.; Skala, D. Alumina/silica supported K_2CO_3 as a catalyst for biodiesel synthesis from sunflower oil. *Bioresour. Technol.* **2009**, *100*, 4690–4696. [CrossRef] [PubMed]
55. Shan, R.; Shi, J.; Yan, B.; Chen, G.; Yao, J.; Liu, C. Transesterification of palm oil to fatty acids methyl ester using K2CO3/palygorskite catalyst. *Energy Convers. Manag.* **2016**, *116*, 142–149. [CrossRef]
56. Liu, H.; Su, L.; Liu, F.; Li, C.; Solomon, U.U. Cinder supported K_2CO_3 as catalyst for biodiesel production. *Appl. Catal. B Environ.* **2011**, *106*, 550–558. [CrossRef]
57. Islam, A.; Taufiq-Yap, Y.H.; Ravindra, P.; Teo, S.H.; Sivasangar, S.; Chan, E.-S. Biodiesel synthesis over millimetric γ-Al_2O_3/KI catalyst. *Energy* **2015**, *89*, 965–973. [CrossRef]
58. Kastner, J.R.; Miller, J.; Geller, D.P.; Locklin, J.; Keith, L.H.; Johnson, T. Catalytic esterification of fatty acids using solid acid catalysts generated from biochar and activated carbon. *Catal. Today* **2012**, *190*, 122–132. [CrossRef]
59. Khan, R.; Mehran, M.T.; Naqvi, S.R.; Khoja, A.H.; Mahmood, K.; Shahzad, F.; Hussain, S. Role of perovskites as a bi-functional catalyst for electrochemical water splitting: A review. *Int. J. Energy Res.* **2020**, *44*, 9714–9747. [CrossRef]
60. Boey, P.-L.; Maniam, G.P.; Hamid, S.A.; Ali, D.M.H. Utilization of waste cockle shell (Anadara granosa) in biodiesel production from palm olein: Optimization using response surface methodology. *Fuel* **2011**, *90*, 2353–2358. [CrossRef]
61. Subramonia Pillai, N.; Kannan, P.S.; Vettivel, S.C.; Suresh, S. Optimization of transesterification of biodiesel using green catalyst derived from Albizia Lebbeck Pods by mixture design. *Renew. Energy* **2017**, *104*, 185–196. [CrossRef]
62. di Bitonto, L.; Reynel-Ávila, H.E.; Mendoza-Castillo, D.I.; Bonilla-Petriciolet, A.; Durán-Valle, C.J.; Pastore, C. Synthesis and characterization of nanostructured calcium oxides supported onto biochar and their application as catalysts for biodiesel production. *Renew. Energy* **2020**, *160*, 52–66. [CrossRef]
63. Leclercq, E.; Finiels, A.; Moreau, C. Transesterification of rapeseed oil in the presence of basic zeolites and related solid catalysts. *J. Am. Oil Chem. Soc.* **2001**, *78*, 1161–1165. [CrossRef]
64. Ibadurrohman, I.A.; Hamidi, N.; Yuliati, L. The role of the unsaturation degree on the droplet combustion characteristics of fatty acid methyl ester. *Alex. Eng. J.* **2022**, *61*, 2046–2060. [CrossRef]
65. Roy, T.; Ágarwal, A.K.; Sharma, Y.C. A cleaner route of biodiesel production from waste frying oil using novel potassium tin oxide catalyst: A smart liquid-waste management. *Waste Manag.* **2021**, *135*, 243–255. [CrossRef] [PubMed]
66. Foroutan, R.; Mohammadi, R.; Razeghi, J.; Ramavandi, B. Biodiesel production from edible oils using algal biochar/CaO/K_2CO_3 as a heterogeneous and recyclable catalyst. *Renew. Energy* **2021**, *168*, 1207–1216. [CrossRef]
67. Daimary, N.; Eldiehy, K.S.H.; Boruah, P.; Deka, D.; Bora, U.; Kakati, B.K. Potato peels as a sustainable source for biochar, bio-oil and a green heterogeneous catalyst for biodiesel production. *J. Environ. Chem. Eng.* **2022**, *10*, 107108. [CrossRef]
68. Chaos-Hernández, D.; Reynel-Avila, H.E.; Mendoza-Castillo, D.I.; Bonilla-Petriciolet, A.; Aguayo-Villarreal, I.A. Functionalization and activation of carbon-based catalysts with KOH and calcium and their application in transesterification to produce biodiesel: Optimization of catalytic properties and kinetic study. *Fuel* **2022**, *310*, 122066. [CrossRef]
69. Jamil, F.; Kumar, P.S.M.; Al-Haj, L.; Myint, M.T.Z.; Al-Muhtaseb, A.H. Heterogeneous carbon-based catalyst modified by alkaline earth metal oxides for biodiesel production: Parametric and kinetic study. *Energy Convers. Manag. X* **2021**, *10*, 100047. [CrossRef]